Functional chicken-liver hydrolysates ameliorate insulin resistance and cognitive decline in streptozotocin-induced diabetic mice

Wei-Yu Yeh,[*,1] Yi-Ling Lin [*,1] Wen-Yuan Yang [†] Chung-Hsi Chou [†,‡] Yi-Hsieng Samuel Wu [*] and Yi-Chen Chen [*,2]

[*]*Department of Animal Science and Technology, National Taiwan University, Taipei City 106, Taiwan;* [†]*Department of Veterinary Medicine, School of Veterinary Medicine, National Taiwan University, Taipei City 106, Taiwan; and* [‡]*Zoonoses Research Center, National Taiwan University, Taipei City 106, Taiwan*

ABSTRACT As part of the slaughtering processing in Taiwan, approximately 10,000 metric tons of broiler livers are produced yearly. However, these livers are regarded as waste. Our team has successfully developed a functional chicken-liver hydrolysate (**CLH**) with several useful activities. It has been reported that there is a positive relationship between diabetes mellitus (**DM**) patients and cognitive decline. To maximize broiler-livers' utilization and add value, we investigated the modulative effects of the CLHs on glucose homeostasis and cognitive decline in streptozotocin (**STZ)** induced diabetic mice. After a 9-wk experiment, CLH supplementation lowered blood glucose by increasing GLUT4 protein expressions in the brains, livers, and muscles of STZ-induced mice ($P < 0.05$). CLHs also enhanced antioxidant capacities in the livers and brains of STZ-induced mice. Amended memory and alternation behavior were tested by using water and Y-maze assays ($P < 0.05$). Besides, STZ-induced mice with CLH supplementation had less contracted neuron bodies in the hippocampus and lower ($P < 0.05$) Aβ depositions in the dentate gyrus area. Less AGE accumulation and apoptosis-related proteins (RAGE, JNK, and activated Caspase 3) in the brains of STZ-induced mice were also detected by supplementing CLHs ($P < 0.05$). In conclusion, the results from this study offer not only scientific evidence on the amelioration of insulin resistance and cognitive decline in hyperglycemia but also add value to this byproduct.

Key words: apoptosis, chicken-liver hydrolysate, cognitive decline, oxidative stress, STZ-induced hyperglycemia

2022 Poultry Science 101:101887
https://doi.org/10.1016/j.psj.2022.101887

INTRODUCTION

Globally, including in Taiwan, poultry meat consumption, especially chicken, has been steadily increasing, driven by the perception that poultry meat is nutritious, convenient, and cheap. Approximately 250 million broilers and 109 million colored broilers (native chickens) were slaughtered in Taiwan in 2020 (Council of Agriculture, Executive Yuan, Taiwan, 2022). The vast quantities of chicken visceral byproducts are a major problem for the poultry industry. Due to an unpleasant odor and health concerns, the broiler liver is regarded as a byproduct or waste product, with associated handling costs. There were around 10,000 metric-ton broiler livers produced yearly in Taiwan. Hence, how to utilize this byproduct is an emergent issue. The U.S. Department of Agriculture (U. S. Department of Agriculture [USDA] 2022) database shows that raw broiler livers contain approximately 16.92% protein. Based on the studies from our research group, a functional chicken-liver hydrolysate (**CLH**) with a specific amino-acid profile/imidazole-ring dipeptide (carnosine and anserine) and some trace mineral irons, that is, manganese (**Mn**) and selenium (**Se**) had been developed (Chou et al., 2014). Meanwhile, its antioxidant effects in D-galactose induction (Chou et al., 2014) and hepatoprotective effects against thioacetamide induction (Chen et al., 2018) and a high-fat diet (Wu et al., 2021) had also been demonstrated. More broiler livers would be utilized when useful biological activities for these protein hydrolysates are demonstrated.

Diabetes mellitus (**DM**) is a metabolic disease that causes hyperglycemia and leads to several complications including nephropathy, cardiovascular disease, sarcopenia, neuropathy, and cognitive decline. According to a report from the World Health Organization (WHO)

Received January 8, 2022.
Accepted March 19, 2022.

[1]These authors contributed equally as co-first authors.

[2]Corresponding author: ycpchen@ntu.edu.tw

(2021), there were a 5% increase in premature mortality from diabetes between 2000 and 2016 and 1.5 million deaths attributable to DM worldwide in 2019 (World Health Organization, 2021). Diabetes could become one of the top ten causes of death by 2030. Diabetes changes energy utilization in several ways, that is, decreased glucose utilization and increased lipolysis and protein breakdown, thus leading the nitrogen loss and ketosis. These changes induce polyphagia, polyuria, and polydipsia (Fournier, 2000). Excessive glucose in the blood activates the polyol pathway, turning glucose into fructose and producing advanced glycation end-products (**AGEs**); meanwhile, NAD^+ is metabolized to NADH, producing reactive oxygen species (**ROS**). Both AGEs and ROS could trigger the receptors of AGEs (**RAGE**) and further induce apoptosis and inflammation in multiple organs, while damage to the brain possibly induces cognitive decline (Niiya et al., 2006). The hippocampus, a part of the memory-storage system in the brain, can be injured by the ROS and hyperglycemia associated with diabetes. It was also reported that the risk of DM patients with cognitive decline is increased (Yaffe et al., 2013). In addition, several reports have indicated that lysine and branched-chain amino acids (**BCAAs**) can reduce blood glucose, increase insulin function, and activate glycogen production (Nishitani et al., 2005).

Our CLHs are rich in antioxidant amino acids (e.g., aromatic amino acids and BCAAs) as well as an imidazole-ring dipeptide (anserine) (Chou et al., 2014). Hence, we tried to investigate the ameliorative effects of CLHs on blood glucose and hyperglycemia-induced cognitive decline in STZ-induced hyperglycemic mice. The Morris water maze and Y-maze assays were used to analyze the cognitive behaviors. Antioxidant capacities, Western blotting (AGE-RAGE signaling pathway), and immunohistochemical staining (β-amyloid) in brain tissues were also used to observe the protective mechanism of CLHs against STZ-induced hyperglycemia and cognitive decline.

MATERIALS AND METHODS

Preparation of CLHs and Total Amino-Acid Profile Analysis

Chicken-liver hydrolysates (**CLHs**) were kindly offered by Great Billion Biotech, Co., Ltd. (New Taipei City, Taiwan), and CLH manufacture was based on the method described in our US patent (Chen et al., 2018). Concerning the quality control of CLH production, the content of hydrolytic amino acids was analyzed by an amino acid analyzer (model L8800, Hitachi High-Technologies Co., Tokyo, Japan) at the Food Industry Research and Development Institute (**FIRDI**, HsinChu City, Taiwan). According to the analysis results (Supplementary Table 1), per 100 g of CLHs, there are 16807.5 mg BCAAs (valine, isoleucine, and leucine: 5346.6, 3590.8, and 7870.1 mg, respectively), 3798.0 mg glycine, 6809.6 mg lysine, 253.7 mg taurine, and 39541.0 mg total essential amino acid (**EAA**).

Animal Treatments

One-hundred male Institute of Cancer Research (**ICR**) mice (approximately 6 wk old; 34−35 g body weight) were purchased from the Laboratory Animal Center of National Taiwan University, Taipei, Taiwan. Mice were housed in an animal room (environment temperature: 24°C, relatively humidity: 60%, light-dark cycle: 12h/12h) and fed with a chow diet (LabDiet 5001, PMI Nutrition International/Purina Mills LLC, Richmond, IN) and distilled water throughout the experimental period. After 1 wk of acclimation, 10 mice were randomly picked up as the Control group. Other mice were injected with STZ (50 mg/kg BW) with nicotinamide (120 mg/kg BW) to induce hyperglycemia for 5 consecutive days. Two days later, 50 mice with fasting blood glucose levels between 235 and 265 mg/dL (13.1−14.7 mmole/L) were selected as hyperglycemic mice and then randomly separated into 5 groups for the subsequent experiment.

The experimental groups were: 1) Control group: Control mice were orally fed with 0.3 mL ddH_2O per mouse; 2) STZ group: STZ-induced hyperglycemic mice were orally fed with 0.3 mL ddH_2O per mouse; 3) CLHs_L group: STZ-induced hyperglycemic mice were orally fed with 0.3 mL ddH_2O per mouse containing 409.46 mg CLHs/kg BW; 4) CLHs_M group: STZ-induced hyperglycemic mice were orally fed with 0.3 mL ddH_2O per mouse containing 818.92 mg CLHs/kg BW; 5) CLHs_H group: STZ-induced hyperglycemic mice were orally fed with 0.3 mL ddH_2O per mouse containing 1223.38 mg CLHs/kg BW; 6) ACTOS group: STZ-induced hyperglycemic mice were orally fed with 0.3 mL ddH_2O per mouse containing 24.67 mg ACTOS/kg BW.

There were 10 mice in all groups, while 2 mice were caged with an ear tag (No. 1 and 2). The experiment lasted for 9 wk. ACTOS was purchased from Takeda Pharmaceutical Co, LTD. (Tokyo, Japan; 30 mg pioglitazone hydrochloride/tablet [approx. 120 mg per tablet]) and used as a positive control agent due to its cognitive protection on STZ treated mice (Liu et al., 2013). The dosages of 1X CLH (low dose) and ACTOS were calculated according to the conversion from the hypoglycemic effects of daily BCAA consumption in a clinical trial (Natarajan Sulochana et al., 2002) and pioglitazone-hydrochloride dosage in adults (1 tablet/day), respectively. The National Taiwan University Institution Animal Care and Use Committee approved this study (IACUU Approval No: NTU106-EL-00092).

Oral Glucose Tolerance Test

The fasting blood glucose level was assayed at the end of the experiment. Before the test, mice fasted overnight while blood glucose levels were detected by using a glucose meter (GM300, Bionime Co. LTD., Taichung City,

Taiwan). The level of oral glucose tolerance (OGTT) (one g glucose/Kg BW, oral gavage) was executed on the 60th day in the experimental period. The diet was completely removed 8 h before starting the assay. The blood glucose level per mouse was detected in 0, 30, 60, 90, and 120 min after the mice were orally administered with one g glucose/kg BW. The trapezoidal rule calculated blood glucose level under the curve (**AUC**) was calculated by the trapezoidal rule (Wu et al., 2021).

Behavior Test (Y Maze and Morris Water Maze)

The Y maze and Morris water maze tests were performed in the experimental period from the 52nd to 58th. The manipulations for these 2 assays were based on the procedures of previous references (Chan et al., 2020; Hakimizadeh et al., 2021).

Y-Maze Test

On the 52nd day in the experimental period, the mice were moved to acclimatize to the room for about 30 min before entering the Y-maze arm apparatus (6 × 25.6 × 14.3 cm, width, length depth) (Diagnostic & Research Instruments Co. LTD., Taipei, Taiwan). The Y-maze arms were divided into 3 areas (a, b, and c). The mice were placed into the end of an arm in the Y maze and allowed to move to other arms within 8 min. An arm entry was only completed if mice's hindlimb paws passed the arm, and the formula calculated alteration: Alternation (%) = Numbers of acute alteration/Total chances to alternation × 100, where total chances to alternation = total arm entries - 2. All behaviors of mice were monitored and assayed by an animal behavior monitor software (Singa Trace mouse II, Diagnostic & Research Instruments Co. LTD., Taipei, Taiwan).

Morris Water Maze

The apparatus for the water maze includes the circular water pool (100 cm in diameter, 80 cm in depth), the movable escape platform (4.3 cm in diameter, 16 cm in height), and video recorder and animal behavior monitor software (Singa Trace mouse II, Diagnostic & Research Instruments Co., Ltd.). Before the experiment, the water was added to a depth of 17 cm with a food coloring agent (Blue, Ever Style Foodstuff Industrial Co. LTD., Taipei, Taiwan, and Black, Precious Investments Co, LTD., Miyazaki, Japan) to reduce the odor trail interference and kept at room temperature (24°C). The pool was divided into 4 equal areas (Z1: right; Z2: opposite; Z3: left; Z4: target) by animal behavior monitor software in videos, while each interior side of the tank wall was pasted with four different visual cues. The experimental procedures were as follows: 1) Mice were moved to the experimental room for water maze at least 30 min before the experiment; 2) Mice were moved into the pool facing the edge of the pool; 3) The mice's behavior was recorded in 60 s. If mice found the escape platform in 60 s, they could stay on it for 15 s. If the mice did not find an escape platform in 60 s, they were moved into the escape platform by the experimenter and stayed for 15 s. After 15 s, the mice were repeated to perform the assay for 60 s.

The day before starting the reference memory test (training trial) (53rd d), the mice were placed into the pool to search the escape platform, placed in the middle of the Z4 quadrant of the pool and emerged 1.0 cm above the water surface. The escape platform was tied with red rubber bands on the top to increase its visibility. On the successive days (54th−57th d), additional water was added into the pool to make the platform 1.5 cm below the water surface, and the mice were placed into the Z1 area of the pool first and placed into Z2 next day by following the counterclockwise direction (Z4 to Z3). Each mouse was placed 4 times, and the escape latency was recorded within 4 d to test the mouse's learning and memory ability. On the 58th day in the experimental period, the escape platform was removed from the pool, and mice were placed into the Z1 area of the pool. Then, the software recorded the swimming speed, the path of swimming, and the number of crossing over the Z4 quadrant within the 60 s.

Sample Collection and Serum Biochemical Values

Before being sacrificed, mice fasted overnight, and blood samples were collected via an orbital sinus. After clotting for 1 h at room temperature, the sera were collected from blood samples by centrifugation at 3,000 × *g*, 4°C for 15 min (Centrifuge, 3700, Kubota Co. Tokyo, Japan) stored at −20°C for future analyses. Brain, heart, liver, kidneys, and hindlimb muscles (including soleus and gastrocnemius muscle) from each mouse were collected, weighed, and then stored at −20° C. The relative organ or muscle sizes (g/100 g BW) were calculated as the following formula: organ or muscle weight (g)/body weight (g) × 100. Concerning the assignment of brain tissues for a further experiment, the brain per mouse was carefully removed, while selected brains per group (No. 1 mouse per cage) were carefully sectioned by the rodent brain matrix (Sunpoint Co., Taoyuan City, Taiwan). The sectioned brain tissues contained the hippocampus and most cerebral cortex areas. For histopathological and immunohistochemical examination, 5-sectioned brain tissues per group were sunk into 10% formaldehyde solution (Merck Millipore Co. Darmstadt, Hesse, Germany). For Western blotting and antioxidative analyses, another 5 brain tissues (No. 2 mouse per cage) were stored in a 2.0 mL tube at −20° C. The AST, ALT, and blood urea nitrogen (**BUN**) levels were analyzed regarding SPOTCHEMTM EZ SP-4430 automatic dry biochemistry analyzer (ARKRAY Inc., Kyoto, Japan). Serum levels of triglyceride (**TG**) and total cholesterol (**TC**) were assayed by commercial kits (TR 210 & CH200, Randox Laboratories LTD., Crumlin, UK). The blood glucose and insulin were

assayed after mice were sacrificed by the glucose meter (GM300, Bionime Co. LTD.) and a commercial kit (EM0260, Wuhan Fine Biotech Co. LTD., Wuhan, China) with the ELISA reader (synergy H1 Hybrid Multi-Mode Microplate Reader, Bio Tek Instruments Inc., Winooski, VT), respectively, while the homeostatic model assessment for insulin resistance (**HOMA-IR**) level was calculated by the formula below:

HOMA-IR = Fasting glucose (mmole/L) × Fasting insulin (mU/L) /22.5 (Liu et al., 2020)

Preparation of Tissue Homogenates

The weighted homogenized brain, liver, and soleus-muscle tissues were mixed with a 9-fold-volume of phosphate buffer saline (PBS, pH 7.4, including 0.25 M sucrose) and homogenized (Polytron, PT-2100, Kinematica AG, Lucerne, Switzerland). Then, the tissue homogenates were centrifuged at 1,000 × *g* at 4°C, and the collected supernatant was stored at −20°C for future analyses. Bio-Rad protein assay kit (catalog # 500-0006; Bio-Rad Laboratories, Inc., Hercules, CA) was applied to measure the protein concentration in the supernatant of each kind of tissue.

Antioxidative Capacity Analyses in Liver and Brain

2-Thiobarbituric acid reactive substances (**TBARS**), reduced glutathione (**GSH**), and trolox equivalent antioxidant capacity (**TEAC**) values in brains and livers, as well as superoxide dismutase (**SOD**) and catalase (**CAT**), were analyzed according to the previous methods (Chan et al., 2020). These were reported in the following units: nmole MDA eq./mg protein, nmole/mg protein, μmole/mg protein, unit/mg protein, munit/mg protein, and unit (liver) or munit (brain)/mg protein, respectively.

Histopathological Analysis and Immunohistochemistry Stain of Brains

All blocks, slides, and stains (H&E and immunohistochemistry staining) of sectioned brain tissues were prepared according to the methods described in our previous study (Tu et al., 2018; Chan et al., 2020). After dehydration and mounting of the slides, photomicrographs of each slide were taken under a LEICA DM500 microscope (Leica Microsystems, Singapore) with an IHD-4600 camera system (Sage Vision Co., LTD, New Taipei City, Taiwan) and Toup View 3.7 software (ToupTek Co., LTD, Hangzhou, China).

For IHC analysis, the heat-induced epitope retrieval was conducted, and tissue sections were incubated with hydrogen peroxide block (TA-060-HP; Thermo Fisher Scientific Inc., Waltham, MA) and protein block solution (TA-060-PBQ; Thermo Fisher Inc.). Then, the slides were incubated with primary antibody (anti-amyloid beta A4 protein, clone MM26-2.1.3, Merck Millipore Co. Darmstadt) (1:100, v/v) for 12 h. Sequentially, the diluted biotinylated secondary antibody buffer was added to the slides for 30 min. The slides were covered by VECTASTAIN Elite ABC reagent (VECTOR Laboratories, Inc., Burlingame, CA) for 30 min. After that, DAB substrate reagent (Cat. No. SK-4100, VECTOR Laboratories, Inc.) was added to the slides for 5 s and washed with tap water immediately. Finally, the counterstain with hematoxylin was added. The slides were also observed under the LEICA DM500 microscope (Leica Microsystems), and photos were taken by using an IHD-4600 camera system (sage Vision Co. LTD.) and Toup view 3.7 software (ToupTek Co. LTD.). The quantification of the relative amounts of beta-amyloid in the brains of experimental mice was measured by using Image J software (National Institutes of Health, Bethesda, MD), and an area with an optical density higher than 0.53 was considered a beta-amyloid deposit.

Western Blotting for Protein Quantification

Before starting the Western blotting, all brain homogenates were diluted to the same concentration. Then, the sample dye with β-mercaptoethanol (Amresco, LLC., Solon, OH) was added into brain homogenates to a ratio of 1:4 (v/v), then heated at 95°C, 10 min. Then, the brain homogenates were stored at −20°C for the Western blotting. The following procedure was done as described in Wu et al. (2021). The information of primary antibiotics used in this study was β-actin (sc-47778, 1:5000 dilutions, Level Biotechnology, Inc., New Taipei City, Taiwan), glucose transporter type 4 (**GLUT4**) polyclonal antibody (#2213, 1:1000 dilution, Cell signaling Technology, Inc, Danvers, MA, USA), advanced glycation end-products (AGEs) polyclonal antibody (bs-1158R, 1:1,000 dilution, Bioss Inc. Woburn, MA), the receptor for AGEs (RAGE) polyclonal antibody (AB9714-l, 1:1,000 dilution, Merck KGaA, Darmstadt, Germany), c-Jun N-terminal kinase (**JNK**) polyclonal antibody (MA5-15183, 1:1,000 dilution, Thermo Fisher Scientific Inc.), and the cleaved Caspase 3 polyclonal antibody (#9664, 1:500 dilution, Cell signaling Technology, Inc. Danvers, MA). The secondary antibody was anti-mouse IgG−horseradish peroxidase (1:10,000 dilution, Thermo Fisher Scientific Inc.). The protein bands were detected by the chemiluminescence (**ECL**) kit (Immobilon Western, Millipore Co. Billerica, MA), under the ChemiDoc MP Imaging System (Bio-Rad CO. Hercules, CA). Image J software (National Institutes of Health) was used to quantify the optical density of protein bands with the value of the β-actin band as a reference, and the intensities of these two bands were used to calculate the ratio of activated Caspase 3 and total Caspase 3.

Statistical Analyses

This was a completely randomized design (**CRD**) experiment. SAS software analyzed the experimental

data (SAS Institute Inc. Cary, NC, USA). When a significant difference was detected at the 0.05 probability level using a one-way analysis of variance (ANOVA), the least significance difference test (**LSD**) was used to distinguish between groups. The data in this study were presented as mean ± standard error of the mean (**SEM**).

RESULTS

Effects of CLHs on Growth Performance, Relative Sizes of Organs, and Serum Biochemical Values of STZ-Induced Hyperglycemic Mice

The body weights of rats among groups were not different ($P > 0.05$) at the beginning of the experiment, but after 8 wk of the experiment, all STZ-induced hyperglycemic groups (STZ, CLH_L, CLH_M, CLH_H, and ACTOS groups) had the lower final body weight than the group without STZ treatment (CON group; $P < 0.05$; Table 1). In the relative organ sizes, the size of the hindlimb muscles in the STZ group was smaller than that of the CON group ($P < 0.05$), but the sizes in the CLH and ACTOS supplemented groups were increased relative to the STZ group ($P < 0.05$) and similar to the CON group ($P > 0.05$). Although the sizes of brain, liver, and kidney in all STZ-induced, hyperglycemic groups were larger than those of CON groups ($P < 0.05$), there was no difference in heart sizes among groups ($P > 0.05$). Regarding serum biochemical values (Table 1), STZ treatment resulted in higher ($P < 0.05$) levels of TG, TC, AST, ALT, BUN, glucose, and insulin in the sera of sacrificed mice, while CLH and ACTOS supplementation reduced or even reversed ($P < 0.05$) serum TG, TC, AST, ALT, BUN, and insulin levels in STZ-induced hyperglycemic mice.

Effects of CLHs on The Blood-glucose Homeostasis in STZ-induced Hyperglycemic Mice

After we measured the fasted serum insulin and glucose levels, STZ treatment apparently resulted in a higher calculated HOMA-IR value ($P < 0.05$), but CLH and ACTOS supplementation could decreases this value ($P < 0.05$; Figure 1A). Concerning OGTT results, CLH and ACTOS supplementation produced lower blood glucose levels in the STZ-induced mice after the immediately oral gavage of glucose (0 min) ($P > 0.05$; Figure 1B). However, the blood glucose levels in all groups increased, and those of STZ treated mice were higher ($P < 0.05$) than that of the CON group (60 and 90 min). After 90 min, CLH and ACTOS supplementation significantly reduced blood glucose levels (Figure 1B). Although STZ treated mice had a larger blood glucose AUC than CON mice, the CLH and ACTOS supplementation groups had significantly lower AUC values than the STZ treated mice ($P < 0.05$; Figure 1C).

Table 1. Effects of chicken-liver hydrolysates on final body weight, relative organ +and hindlimb muscle sizes, serum biochemical values of experimental mice, and antioxidant capacities in livers and brains of experimental mice.

Groups	CON	STZ	CLH_L	CLH_M	CLH_H	ACTOS
Final body weight (g)*	37.64±0.70^{a}	31.77±0.92^{b}	30.94±0.76^{b}	32.24±0.78^{b}	31.69±0.43^{b}	32.26±0.75^{b}
Relative organ sizes (g/100 g BW)*						
Brain	1.24±0.04^{b}	1.55±0.05^{a}	1.48±0.05^{a}	1.59±0.05^{a}	1.57±0.04^{a}	1.59±0.05^{a}
Heart	0.50±0.02^{a}	0.46±0.02^{a}	0.45±0.01^{a}	0.47±0.02^{a}	0.49±0.02^{a}	0.46±0.02^{a}
Liver	4.51±0.17^{b}	5.69±0.16^{a}	5.72±0.11^{a}	5.56±0.14^{a}	5.78±0.13^{a}	5.77±0.12^{a}
Kidney	1.57±0.06^{b}	1.94±0.08^{a}	1.81±0.05^{a}	1.86±0.07^{a}	1.90±0.04^{a}	1.94±0.04^{a}
Hindlimb muscle	7.75±0.22^{a}	6.72±0.45^{b}	8.08±0.13^{a}	7.45±0.16^{a}	7.84±0.09^{a}	7.78±0.11^{a}
Serum biochemical values*						
TG (mg/dL)	88.40±5.48^{b}	118.15±4.51^{a}	92.89±8.26^{b}	83.53±6.50^{b}	84.05±6.55^{b}	85.55±11.74^{b}
TC (mg/dL)	109.25±5.04^{b}	136.59±8.17^{a}	118.19±6.28^{b}	113.40±9.57^{b}	109.98±4.07^{b}	101.98±5.60^{b}
AST (IU/L)	52.00±3.30^{c}	150.50±7.61^{a}	111.70±10.75^{b}	103.90±11.82^{b}	105.50±9.64^{b}	115.90±11.84^{b}
ALT (IU/L)	28.00±2.82^{c}	65.90±7.29^{a}	36.80±4.81^{b}	35.90±6.23^{b}	37.00±5.10^{b}	40.90±4.20^{b}
BUN (mg/dL)	17.40±0.67^{c}	26.20±1.68^{a}	22.00±0.91^{b}	22.92±1.47^{b}	23.56±0.92^{b}	22.10±1.39^{b}
Glucose (mmole/L)	8.45±0.22^{c}	30.90±0.73^{a}	24.90±1.05^{b}	26.67±1.29^{b}	26.48±1.04^{b}	25.64±1.46^{b}
Insulin (mU/L)	12.87±0.35^{c}	34.42±2.00^{a}	18.90±2.27^{b}	19.22±2.25^{b}	20.23±1.12^{b}	24.47±1.35^{b}
Liver antioxidant capacities*						
TBARS (nmole MDA eq./mg protein)	18.00±1.02^{b}	27.87±1.41^{a}	23.75±2.00^{a}	26.36±2.01^{a}	26.83±1.59^{a}	24.78±0.95^{a}
Reduced GSH (nmole/mg protein)	71.14±10.96^{a}	30.87±4.30^{d}	39.47±2.28^{cd}	56.92±5.47^{ab}	52.92±3.33^{bc}	52.94±3.49^{bc}
TEAC (μmole/mg protein)	0.15±0.01^{a}	0.07±0.01^{d}	0.09±0.01^{cd}	0.12±0.01^{bc}	0.12±0.01^{b}	0.10±0.002^{bc}
SOD (unit/mg protein)	5.10±0.51^{a}	2.88±0.30^{c}	3.75±0.39^{bc}	4.56±0.40^{ab}	4.50±0.41^{ab}	4.37±0.30^{ab}
Catalase (munit/mg protein)	332.17±25.79^{a}	194.04±23.25^{d}	219.29±19.02^{cd}	309.53±21.28^{ab}	301.65±23.80^{ab}	267.94±12.44^{bc}
GPx (unit/mg protein)	12.67±0.86^{a}	9.42±0.61^{b}	10.73±0.70^{ab}	13.58±0.98^{a}	11.93±0.80^{a}	12.68±0.78^{a}
Brain antioxidant capacities*						
TBARS (nmole MDA eq./mg protein)	72.31±6.55^{b}	112.66±16.78^{a}	87.77±12.35^{ab}	70.27±3.59^{b}	74.89±1.36^{b}	62.88±5.46^{b}
Reduced GSH (nmole/mg protein)	155.66±9.67^{a}	58.86±13.33^{c}	99.65±8.17^{b}	111.35±8.35^{b}	111.94±4.58^{b}	115.81±19.13^{b}
TEAC (μmole/mg protein)	1.85±0.12^{a}	1.30±0.12^{b}	1.94±0.23^{a}	1.79±0.13^{a}	1.94±0.11^{a}	1.79±0.11^{a}
SOD (unit/mg protein)	5.83±0.66^{a}	2.40±0.41^{c}	4.88±0.45^{ab}	3.95±0.25^{b}	4.71±0.21^{ab}	4.660.77^{ab}
Catalase (munit/mg protein)	4.98±0.64^{a}	2.42±0.55^{b}	4.83±0.44^{a}	4.51±0.28^{a}	4.64±0.47^{a}	4.43±0.63^{a}
GPx (munit/mg protein)	117.41±2.90^{a}	74.47±3.68^{b}	136.60±5.12^{a}	117.71±7.26^{a}	110.12±8.67^{a}	120.34±14.40^{a}

*Data are given as mean ± SEM (n = 10).

^{abcd}Mean values without a common letter in each test parameter indicate a significant difference ($P < 0.05$).

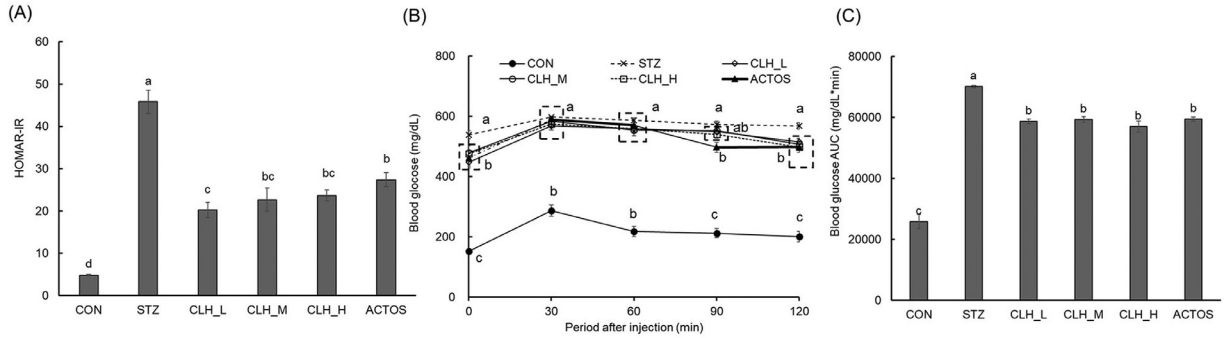

Figure 1. Effects of chicken-liver hydrolysates on (A) homeostasis model assessment (HOMA-IR), (B) oral glucose tolerance test, and (C) blood glucose AUC of the experimental mice. * Data are given as mean ± SEM (n = 10). ** Data points in each test period after injection, or data bars in blood glucose AUC and HOMAR-IR, respectively, without a common letter indicate a significant difference ($P < 0.05$).

Effects of CLHs on The Antioxidant Capacities in Livers and Brains of STZ-Induced Hyperglycemic Mice

The antioxidant capacities in livers and brains of experimental mice are shown in Table 1. STZ treatment increased ($P < 0.05$) TBARS values in both livers and brains. There were lower levels of reduced GSH and TEAC in the liver and brain than those of the CON group ($P < 0.05$). Although no changes on liver TBARS values were assayed by supplementing CLH or ACTOS ($P > 0.05$), they both decreased brain TBARS values ($P < 0.05$), which are similar ($P > 0.05$) to that of the CON group. By contrast, the decreased levels of reduced GSH and TEAC in the livers and brains of STZ-induced mice were amended ($P < 0.05$) by CLH or ACTOS supplementation, except in the livers of the low-dose CLH supplemented group ($P > 0.05$). Concerning the activities of antioxidant enzymes, all STZ treated groups had lower ($P < 0.05$) SOD, CAT, and glutathione peroxidase (**GPx**) activities in the liver and brain compared to those of the CON group. Similarly, CLH or ACTOS supplementation increased ($P < 0.05$) those activities in STZ treated mice. Those reversed effects even demonstrated similar ($P > 0.05$) activities as those of the CON group, except the SOD activity of CLH_L and CLH_M group in the liver and brain ($P > 0.05$), respectively, against that of the CON group.

Effects of CLHs on The Spatial Learning and Memory Abilities of STZ-Induced Hyperglycemic Mice

The results of the Morris water maze are shown in Figure 2. On days 1 and 2, no differences among groups

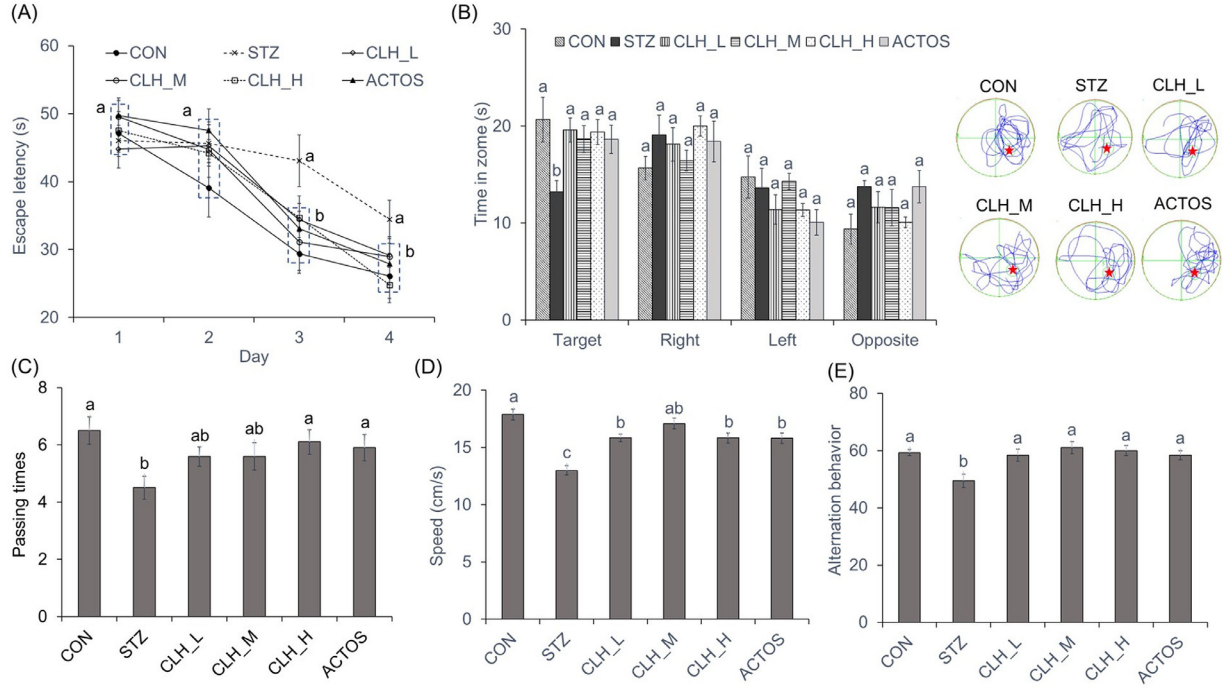

Figure 2. Effects of chicken-liver hydrolysates on (A) the escape latency during the reference memory test, (B) spending period in each zone and the swimming routes (: the place of the removed escape platform), (C) the numbers of crossing over the target zone, (D) the swimming speed during the probe test in Morris water maze, and (E) alternation behavior in Y maze of the experimental mice. * Data are given as mean ± SEM (n = 10). ** Data points in each test day or data bars in each test zone or parameter without a common letter indicate a significant difference ($P < 0.05$).

on escape latency were recorded ($P > 0.05$; Figure 2A). However, after d 3, the STZ group showed significantly longer escape latencies than the CON group ($P < 0.05$), but CLH or ACTOS supplementation shortened the escape latencies in STZ-induced hyperglycemic mice($P < 0.05$), which were similar to that of the CON group. Furthermore, the results of the probe test are shown in Figures 2B, C, and D. The STZ group spent less time in the target zone than the CON group ($P <0.05$), while the CLH and ACTOS supplemented groups spent longer in the target zone than the STZ group ($P <0.05$) (Figure 2B). According to the illustrations of swimming routes (Figure 2B), the STZ group showed an irregular swimming route compared to CON and CLH or ACTOS supplemented groups, which tended to close the target zone. Similar results were also observed in the passing times of experimental mice in the target zone (Figure 2C). Besides, the STZ group had a lower ($P < 0.05$) swimming speed than the CON group, while CLH or ACTOS supplemented groups had a higher ($P < 0.05$) swimming speed than the STZ group (Figure 2D). Concerning the result of the Y maze (Figure 2E), the STZ group had weaker ($P < 0.05$) alternation behavior than other groups, and there was no difference among the CON and CLH or ACTOS supplemented groups ($P > 0.05$).

Effects of CLHs on The Histological Pathologies and β-amyloid (Aβ) Depositions in The Hippocampus of STZ-Induced Hyperglycemic Mice

Hematoxylin and eosin (**H&E**) staining revealed the morphological characteristics of the dentate gyrus area in the hippocampus (Figure 3A). The STZ group had more contracted neuron bodies stained by hematoxylin in the granule cell layer and subgranular zone (dark arrow) than the CON group. Although the CLH or ACTOS® supplemented groups still accumulated contracted neuron bodies in the dentate gyrus area, less accumulation was observed than in the STZ group.

Moreover, Aβ accumulation in the hippocampus was observed by immunochemical staining (Figure 3B). In the STZ and ACTOS groups, there were more Aβ deposits, which were indicated by the dark arrow in the dentate gyrus area, while the deposit was decreased in CLH

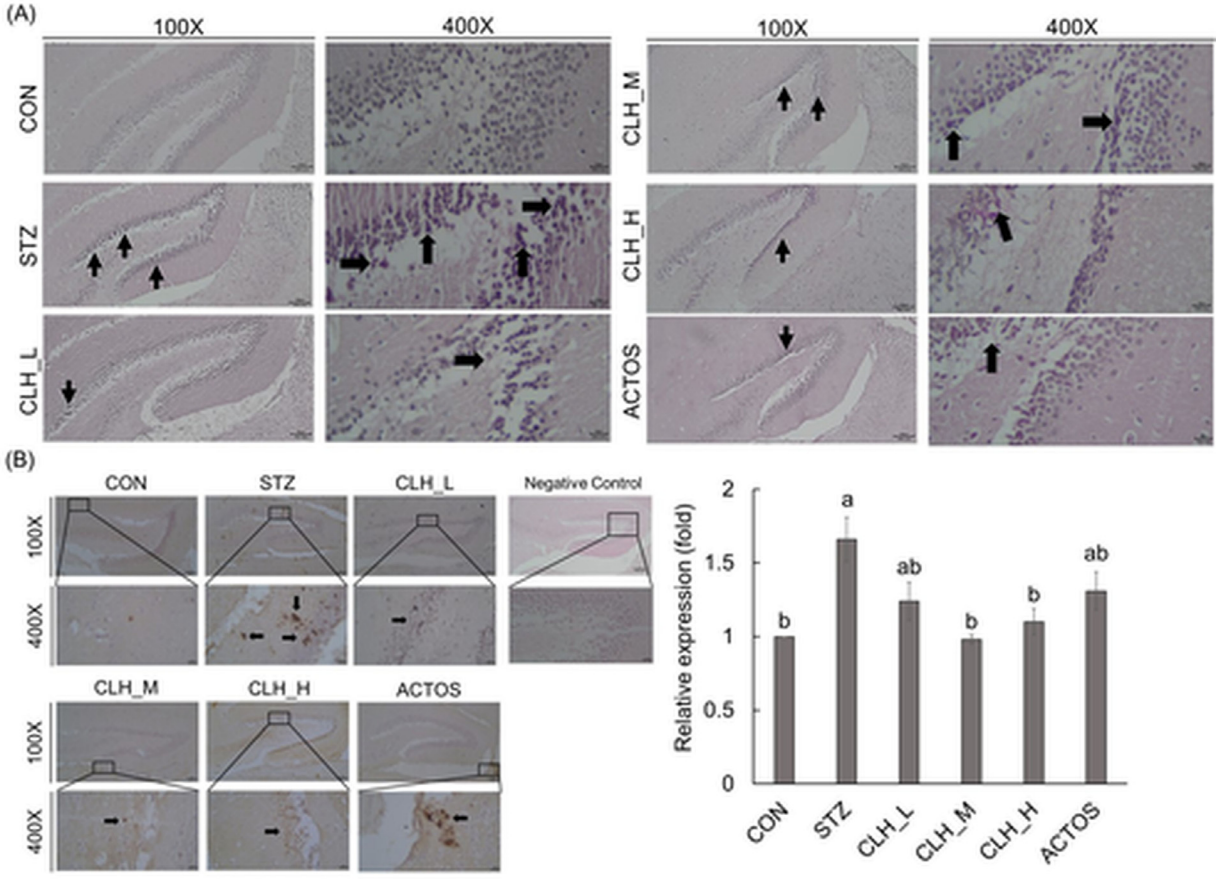

Figure 3. (A) Morphological features of the dentate gyrus area in mouse hippocampus from (A) CON, (B) STZ, (C) CLH_L, (D) CLH_M, (E) CLH_H, and (F) ACTOS groups were evaluated by using H&E staining. The presence of dark neurons is characterized by contracted neuron bodies. (B) The effects of CLHs on the β-amyloid accumulation in the dentate gyrus area of mouse hippocampus were shown as brown spots using DAB-revealed horseradish peroxidase immunohistochemistry and quantification of the relative amount of beta-amyloid in the brains of experimental mice. Scale bar: 100 and 20 μm. * Data are given as mean ± SEM (n = 5), and data bars without the common letter indicate a significant difference ($P < 0.05$). ** The normal dentate gyrus area in the mouse hippocampus without using immunohistochemistry was shown as a negative Control (B). *** The relative amount of β-amyloid in STZ, CLH_L, CLH_M, CLH_H, and ACTOS groups were expressed relative to the average values for mice in the CON group, which was set to 1.0.

or ACTOS supplemented groups. In the quantification of the relative amounts of Aβ (Figure 3B), the STZ group also showed a higher ($P < 0.05$) Aβ deposit level than the CON group, while the supplementation of medium and high doses of CLHs resulted in less ($P < 0.05$) Aβ deposits compared to the STZ group.

Effects of CLHs on The Apoptosis Related Protein Expressions and AGE Products in The Hippocampus as Well as GLUT 4 Protein Expressions in Hindlimb and Livers of STZ-Induced Hyperglycemic Mice

By Western blotting, the protein expressions of RAGE, JNK, and activated Caspase 3 in brains of the STZ group were higher than those in the CON group ($P < 0.05$; Figure 4A). However, CLH or ACTOS supplementation decreased those protein expressions in the brains of STZ-induced hyperglycemic mice ($P < 0.05$). An increased amount of AGE products in brains was obtained in the STZ group compared to that in the CON group ($P < 0.05$), but ACTOS supplementation decreased the amount of AGE products in brains in STZ-induced hyperglycemic mice ($P < 0.05$; Figure 4B). Although there was only a tendency toward fewer AGE products in STZ injected mice co-treated with CLHs, the number of AGE products in the brains of CLH_M and CLH_H groups was not different from the CON group ($P > 0.05$). Concerning the ability of glucose transport to tissues, the lowest ($P < 0.05$) GLUT 4 protein expressions in the brain, hindlimb muscle, and livers were measured in the STZ group, but CLH and ACTOS supplementation upregulated GLUT 4 protein expressions ($P < 0.05$; Figures 4A, 4C, and 4D).

DISCUSSION

DM is a major metabolic disease that causes hyperglycemia and leads to several complications, including nephropathy, cardiovascular disease, sarcopenia, neuropathy, and cognitive decline. The small skeletal muscle in STZ-induced mice is observed due to induced atrophy of the AGEs (Chiu et al., 2016), while the enlarged liver in STZ-induced mice could be caused by the superabundant triglyceride accumulation (Zafar and Naqvi, 2010). The organ damage in hyperglycemic animals is mostly caused by the accumulation of free radicals in the body. In diabetic animals, in addition to increased serum AST and ALT levels in hyperglycemic animals, BUN (a marker for nephropathy) is also increased due to the decrease of the glomerular filtration rate (Chiu et al., 2016). It has also been reported that BCAAs could increase insulin sensitivity while reducing the serum glucose and insulin levels in Otsuka Long-Evans Tokushima fatty (**OLETF**) rats (Kuzuya et al., 2008) and STZ-induced rats (Zhu et al., 2021). The hyperglycemia-induced ROS also induces the increases of serum AST and ALT. Supplementing CLHs or ACTOS could improve diabetes-related serum biochemical values in this study. It has been proposed that insulin resistance results in the lower descending speed of blood glucose, and the AUC level under OGTT is increased in diabetic rats (Marthandam et al., 2019).

We propose that the improvement of blood glucose in STZ injected mice by supplementing CLH might be due to the BCAA contents (isoleucine + leucine + valine = 16,807.5 mg/100 g dried CLHs) (Supplementary Table 1). Besides, CLHs also contains glycine (3,798.0 mg/100 g dried CLHs) and lysine (6,809.63 mg/100 g dried CLHs). Li et al. (2019) reported that the blood glucose level was decreased in STZ-induced hyperglycemic rats after 45 d of the administration of glycine (250 and 500 mg/kg BW), and they also found that aldose reductase, which plays a critical role in the production of AGEs in the lens, could be decreased by the glycine administration. The hypoglycemic effect of ACTOS is due to increased insulin sensitivity, thus decreasing blood-glucose levels (Liu et al., 2013). Based on the results (Table 1 and Figure 1), our

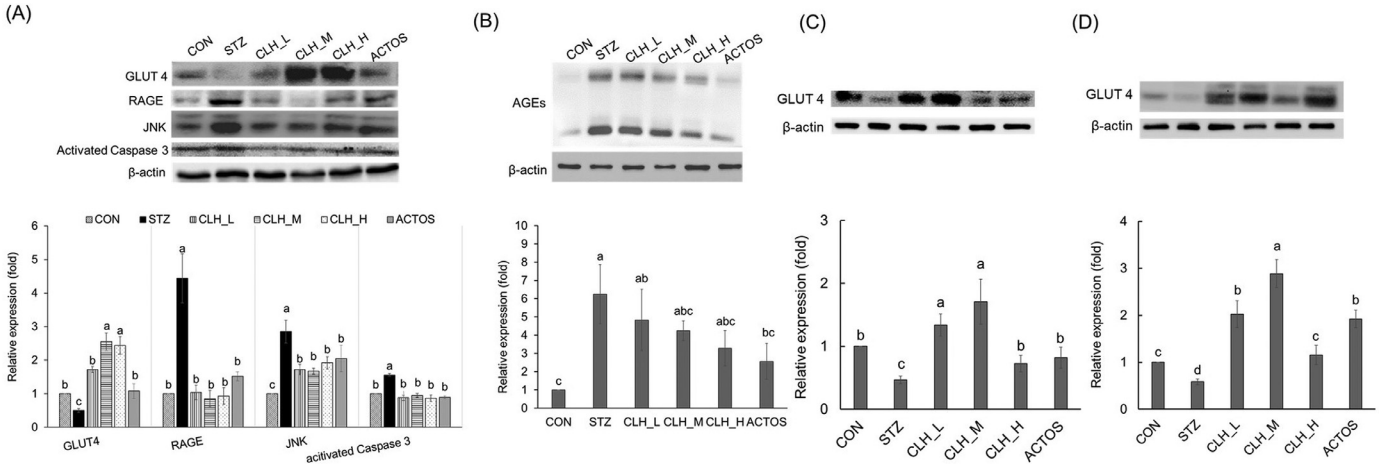

Figure 4. Effect of chicken-liver hydrolysates on protein expressions of (A) GLUT4, RAGE, JNK, and activated Caspase 3, and (B) AGEs in the brains, as well as GLUT4 protein levels in (C) hindlimb muscles and (D) livers of the experimental mice. * Data are given as mean ± SEM (brain, n = 5; hindlimb muscle and liver, n = 10). ** Protein expressions in STZ, CLH_L, CLH_M, CLH_H, and ACTOS groups were expressed relatively to the average values for that in the CON group, which was set to 1.0. Data bars without a common indicate a significant difference ($P < 0.05$).

CLHs demonstrated similar hypoglycemic effects in STZ injected mice as ACTOS, which might be due to improving the insulin sensitivity in STZ injected hyperglycemic mice. Besides, GLUT 4 is a key determinant of glucose homeostasis, which permits the facilitated diffusion of serum glucose into muscle, adipose, liver and brain cells (Kairupan et al., 2019), and BCAAs can stimulate the GLUT 4 activity and insulin sensitivity, thus decreasing blood glucose levels (Nishitani et al., 2005), and there is the amount of BCAAs in our CLHs (Supplementary Table 1). Isoleucine supplementation could potentially increase muscle growth and intestinal development by enhancing local glucose uptake in animals and human beings via upregulations of the intestinal and muscular GLUT 1 and GLUT 4 expressions (Zhang et al., 2016). Hence, the increased GLUT 4 protein expressions in the brain, liver, and hindlimb muscle of STZ-induced hyperglycemic mice by supplementing our CLHs should high correspond to the improved insulin sensitivity (Figure 1 vs. Figure 4) and also contribute to the increased size of hindlimb muscle (Table 1 vs. Figure 4C), which might result from the contents of BCAAs (16,807.5 mg/100 g dried CLHs), glycine (3,798.0 mg/100 g dried CLHs), and lysine (6,809.6 mg/100 g dried CLHs).

Excessive glucose in hyperglycemic conditions can activate more ROS produced through an electron transport chain in mitochondria. Besides, ROS are also produced by activated RAGEs, thus triggering NF-κB and Caspase 3, inducing inflammation and apoptosis in brains of hyperglycemic condition (Tu et al., 2018; Chan et al., 2020). It has been reported that protein hydrolysates or peptides with special specific amino acids have antioxidant activities (e.g., aromatic amino acids [Zheng et al., 2020], histidine [Wu et al., 2003], and aspartic acid [Qian et al., 2008]). Moreover, dietary glycine supplements could reduce the oxidative stress in the livers by increasing the content of reduced GSH and glutamylcysteine and the activities of γ-glutamylcysteine synthetase (**γ-GCS**) in the sucrose induced hyperglycemic rats (El-Hafidi et al., 2018). Taurine could ameliorate diabetes by controlling advanced glycation end-product, improving insulin secretion, and avoiding diabetes-induced complications (e.g., brain damage [neuropathy], retinopathy, liver damage [steatohepatitis], vascular/heart problems) that partially result from its protection against oxidative stress (Inam-U-Llah et al., 2018). In addition, Campos-Bedolla et al. (2014) indicated that those antioxidant amino acids could pass through the blood-brain barrier (**BBB**) via a specific transporter.

In our previous study, we found that CLH supplementation (250 mg/kg BW) could decrease TBARS levels, increase reduced GSH and TEAC levels, as well as reverse SOD, CAT, and GPx activities in the liver and brain of D-galactose-treated mice (1.2 g D-galactose/kg BW) (Chou et al., 2014). Based on the amino acid profile analysis in our CLHs (Suppl. Table 1), 100 g of dried CLHs contains 3,053.0 mg of tyrosine, 1,773.7 mg of histidine, 632.4 mg of tryptophan 3,374.1 mg of phenylalanine, 5,947.5 mg of aspartic acid, 3798.0 mg of glycine, and 253.7 mg of taurine. Hence, we speculate that those antioxidant amino acids contribute to the antioxidant ability in STZ-induced hyperglycemic mice

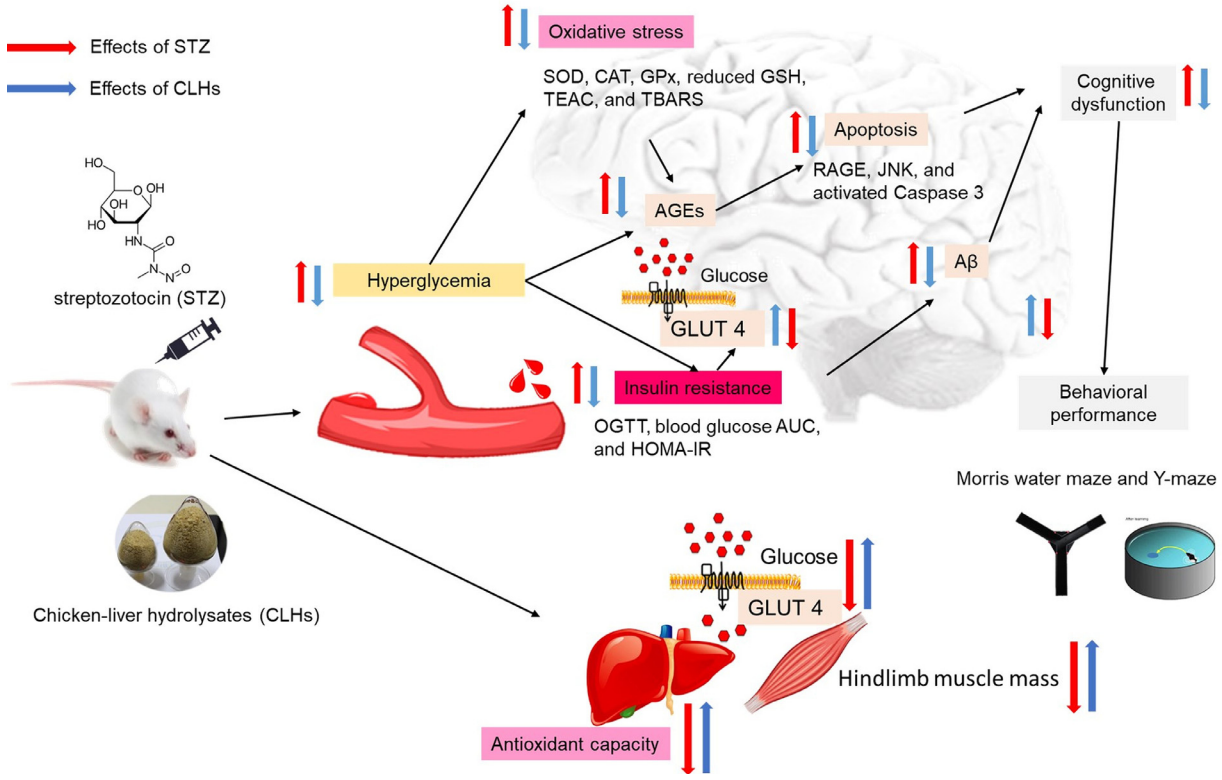

Figure 5. The ameliorative mechanism of chicken-liver hydrolysates (CLHs) on the hyperglycemia and cognitive dysfunction in the STZ treated mice.

(Supplementary Table 1 and Table 1). Yaffe et al. (2013) reported that the risk of cognitive decline is increased in DM patients. Liu et al. (2020) proposed that the hyperglycemic condition might injure the hippocampus and cause cognitive decline. These authors report that hyperglycemic rats have significantly increased escape latency to find the escape platform, interfered with the swimming route in the reference memory test, and decreased the period in the area of the escape platform in the probe test. Y maze is also used in examining the spontaneous alternation behavior indicating the ability of short-term spatial memory performance in the hyperglycemic animals (Nitta et al., 2002). Nitta et al. (2002) reported that STZ-induced hyperglycemic rats have the lower spontaneous alternation behavior due to the synapse dysfunction in the hippocampus and cortex of diabetic rats. It was reported that taurine supplementation could improve D-galactose-treated mice's impaired behavior performance in the Morris water maze via enhancing antioxidant and anti-inflammatory effects in brains (Tu et al., 2018). Taurine is also assayed in our CLHs (253.7 mg/100 g dried CLHs) (Supplementary Table 1). Moreover, there are antioxidant amino acids in our CLHs other than those mentioned in the previous section. Hence, it could be hypothesized that the antioxidant amino acids in our CLHs amend the oxidative stress in STZ-induced hyperglycemic conditions and then improve the behavior performance (Morris water maze and Y maze) (Supplementary Table 1, Table 1, and Figure 2). In addition, our previous study reported that the CLHs also contain selenium (Se) and manganese (Mn) which are coenzymes of 2 antioxidant enzymes,SOD, and GPx, respectively (Chou et al., 2014). Besides, an increased oxidative level in brains resulted in cognitive dysfunction (Tu et al. 2018; Chan et al., 2020). Therefore, it could be hypothesized that the specific amino-acid profile and trace elements (Se and Mn) in CLHs improve oxidative status in the brains of STZ-induced diabetic mice, thus ameliorating cognitive decline.

Neurogenesis is always taking place in the dentate gyrus of the hippocampus while the proliferation of granule neuron cells in the hippocampus is necessary for the formation of memory and learning, and a diabetic condition reduces proliferation, increases neuron apoptosis in the hippocampus, and induces memory and learning impairment (Jackson-Guilford et al., 2000). An STZ administration (45 mg/kg BW) can induce the activation of Caspase 3 in the cerebral cortex and hippocampus of male Wistar rats, while in STZ-induced rats, the escape latency is increased, and the spent period on the target area is decreased in the Morris water maze (Kuhad et al., 2009). Besides, the Aβ deposit, which is cleaved from Aβ precursor protein and mainly contains peptides of 40 and 42, is one of the major pathological hallmarks in Alzheimer's and diabetes mellitus (Zhao et al., 2004). Due to insulin resistance, the protein expression of the insulin-degrading enzyme (**IDE**), which also can degrade Aβ in the hippocampus and cerebral cortex, is reduced (Zhao et al., 2004). The Aβ deposit is also increased by oxidative stress, which stimulates the levels of amyloid-beta precursor protein (**APP**) and Aβ related protein, such as beta-site APP-cleaving enzyme (**BACE**) and γ-secretase (Golde, 2003). It was reported that the Aβ protein level is decreased in the brains of D-galactose-treated mice by administering a functional egg chalaza hydrolysate via reducing the oxidative stress in the brains (Chan et al., 2020). The effects of CLHs on the decrease of Aβ might result from the ability to decrease insulin resistance (Figure 1) and brain oxidative stress (Table 1). CLHs also are rich in arginine (5,198.6 mg/100 g dried CLHs), which are reported to have the ability to interrupt the interaction of Aβ (Kawasaki and Kamijo, 2012). The ability of our CLHs to decrease the Aβ formation should justify further investigation. The AGEs are produced via the reaction of reducing sugar and protein, which also makes protein dysfunctional, and AGEs could activate the RAGE, the receptor of AGE, thus upregulating TNFα and IL-6, which further cause inflammatory responses. They also reported that the AGEs and activated RAGE are highly related to cell apoptosis, where the gene or protein expressions of apoptosis-related factors are enhanced (e.g., Bax, Caspase 3, and Caspase 9; Tu et al., 2018; Chan et al., 2020). It was also observed that apoptosis occurred in the hippocampus of STZ-induced hyperglycemic rats where Caspase 3 expression is stimulated. Thus, it is important to improve cognitive decline by downregulating the brain's apoptosis (Jafari Anarkooli et al., 2008). Meanwhile, the time to escape to the target platform was decreased, and time spent in the target area was increased in the Morris water maze.

Moreover, inhibition of AGE formation might be another way to reduce the AGEs induced apoptosis. Arginine could interfere with the formation of AGEs by its guanidine groups, which could block the carbonyl groups in AGEs formation (Lubec et al., 1990). Taurine can also inhibit the AGEs formation in oxidative injured brains (Tu et al., 2018). Therefore, we propose that the contents of arginine and taurine in our CLHs play a crucial role in anti-AGEs formation in STZ-induced hyperglycemic mice. In the antioxidant capabilities, CLHs contain aromatic amino acids and aspartic acid, playing as a chelator and hydrogen donor (Qian et al., 2008; Zheng et al., 2020). Therefore, our CLHs could decrease the amount of AGEs produced and inhibit the protein expressions of RAGE, JNK, and the relative ratio of activated Caspase 3 and total Caspase 3 in the brains of STZ-induced hyperglycemic mice, thus improving the oxidative-stress induced cognitive decline.

CONCLUSIONS

The ameliorative effects of this functional CLH on insulin resistance and cognitive decline in STZ-induced hyperglycemic mice have been summarized in Figure 5. The CLH supplementation significantly upregulated the GLUT 4 protein expressions in the brain, liver, and

hindlimb muscle reduced the level of blood glucose and attenuated the oxidative damage in the brain of STZ treated mice. With the decrease of blood glucose and oxidative stress in STZ treated mice, AGEs accumulation and AGEs/RAGE/Caspase 3 apoptotic pathway could be decreased or downregulated by supplementing CLHs. The Aβ deposit and contracted neuron bodies in the hippocampus of STZ treated mice were also decreased by supplementing CLHs. Moreover, CLH supplementation improved the behavioral performance in the Morris water maze (memory abilities) and Y maze (alternation abilities) of STZ-treated mice. In addition, the increased muscle mass of hindlimb legs was also observed in the STZ-induced hyperglycemic mice cotreated with CLHs, which enhances the swimming speed in the probe test of the Morris water maze. Hence, this study aims not only to develop CLHs as a potential functional-food ingredient that can improve insulin resistance, oxidative pressure, and cognitive decline in hyperglycemia but also maximize the utilization of poultry byproducts, thus decreasing the environmental burden of handling agricultural byproducts in the chicken industry.

ACKNOWLEDGMENTS

We acknowledge funding of this research from the Great Billion Biotech, Co., Ltd. (New Taipei City, Taiwan), and partially from the Ministry of Science and Technology, Taiwan (Project: MOST 109-2313-B-002-007-MY3) and Council of Agriculture, Executive Yuan, Taiwan (Project: 110AS-17.1.4-ST-a1 and 111AS-2.2.2-AD-U1(1))

Authorship contribution statement: **Wei-Yu Yeh:** Methodology, Data curation, Data statistical analysis, Writing original draft. **Yi-Ling Lin:** Data collection, Formal analysis, Investigation, Writing original draft. **Wen-Yuan Yang:** Formal analysis, Investigation, Supervision, Revising the draft. **Chung-Hsi Chou:** Supervision, Revising the draft. **Yi-Hsieng Samuel Wu:** Methodology, Revising the draft. **Yi-Chen Chen:** Project administration, Methodology, Conceptualization, Supervision, Writing - review & editing.

DISCLOSURES

There are no conflicts of interest to declare.

SUPPLEMENTARY MATERIALS

Supplementary material associated with this article can be found in the online version at doi:10.1016/j.psj.2022.101887.

REFERENCES

Campos-Bedolla, P., F. R. Walter, R. Veszelka, and M. A. Deli. 2014. Role of the blood-brain barrier in the nutrition of the central nervous system. Arch. Med. Res. 45:610–638.

Chan, C. J., J. K. Tseng, S. Y. Wang, Y. L. Lin, Y. H. S. Wu, J. W. Chen, and Y. C. Chen. 2020. Ameliorative effects of functional chalaza hydrolysates prepared from protease-A digestion on cognitive dysfunction and brain oxidative damages. Poult. Sci. 99:2819–2832.

Chen, Y. C., P. J. Chen, and S. Y. Tai. 2018. Composition of chicken liver hydrolysates and method for improving alcohol metabolism, as well as preventing and treating liver fibrosis. Inventor; National Taiwan University, assignee. USA patent: US10,105,400B2.

Chiu, C. Y., R. S. Yang, M. L. Sheu, D. C. Chan, T. H. Yang, K. S. Tsai, C. K. Chiang, and S. H. Liu. 2016. Advanced glycation end-products induce skeletal muscle atrophy and dysfunction in diabetic mice via a RAGE-mediated, AMPK-down-regulated, Akt pathway. J. Pathol. 238:470–482.

Chou, C. H., S. Y. Wang, Y. T. Lin, and Y. C. Chen. 2014. Antioxidant activities of chicken liver hydrolysates by pepsin treatment. Int. J. Food Sci. Technol. 49:1654–1662.

Council of Agriculture, Executive Yuan, Taiwan. 2022. Agricultural production: 2. livestock production. Accessed Mar. 2022. https://eng.coa.gov.tw/ws.php?id=2505655

El-Hafidi, M., M. Franco, A. R. Ramírez, J. S. Sosa, J. A. P. Flores, O. L. Acosta, M. C. Salgado, and C. Cardoso-Saldaña. 2018. Glycine increases insulin sensitivity and glutathione biosynthesis and protects against oxidative stress in a model of sucrose-induced insulin resistance. Oxid. Med. Cellul. Longev. 2018:2101562.

Fournier, A. 2000. Diagnosing diabetes. A practitioner's plea: keep it simple. J. Gen. Intern. Med. 15:603–604.

Golde, T. E. 2003. Alzheimer disease therapy: can the amyloid cascade be halted? J. Clin. Invest. 111:11–18.

Hakimizadeh, E., M. Zamanian, L. Giménez-Llort, C. Sciorati, M. Nikbakhtzadeh, M. Kujawska, A. Kaeidi, J. Hassanshahi, and I. Fatemi. 2021. Calcium dobesilate reverses cognitive deficits and anxiety-like behaviors in the D-galactose-induced aging mouse model through modulation of oxidative stress. Antioxidants 10:649.

Inam-U-Llah, F. Piao, R. M. Aadil, R. Suleman, K. Li, M. Zhang, P. Wu, M. Shahbaz, and Z. Ahmed. 2018. Ameliorative effects of taurine against diabetes: a review. Amino Acids 50:487–502.

Jackson-Guilford, J., J. D. Leander, and L. K. Nisenbaum. 2000. The effect of streptozotocin-induced diabetes on cell proliferation in the rat dentate gyrus. Neurosci. Lett. 293:91–94.

Jafari Anarkooli, I., M. Sankian, S. Ahmadpour, A. R. Varasteh, and H. Haghir. 2008. Evaluation of Bcl-2 family gene expression and caspase-3 activity in hippocampus STZ-induced diabetic rats. Exp. Diabetes Res. 2008:638467.

Kairupan, T. S., K. C. Cheng, A. Asakawa, H. Amitani, T. Yagi, K. Ataka, N. T. Rokot, N. H. Kapantow, I. Kato, and A. Inui. 2019. Rubiscolin-6 activates opioid receptors to enhance glucose uptake in skeletal muscle. J. Food Drug Anal. 27:266–274.

Kawasaki, T., and S. Kamijo. 2012. Inhibition of aggregation of amyloid β42 by arginine-containing small compounds. Biosci. Biotechnol. Biochem. 76:762–766.

Kuhad, A., M. Bishnoi, V. Tiwari, and K. Chopra. 2009. Suppression of NF-$\kappa\beta$ signaling pathway by tocotrienol can prevent diabetes associated cognitive deficits. Pharmacol. Biochem. Behav. 92:251–259.

Kuzuya, T., Y. Katano, I. Nakano, Y. Hirooka, A. Itoh, M. Ishigami, K. Hayashi, T. Honda, H. Goto, Y. Fujita, R. Shikano, Y. Muramatsu, G. Bajotto, T. Tamura, N. Tamura, and Y. Shimomura. 2008. Regulation of branched-chain amino acid catabolism in rat models for spontaneous type 2 diabetes mellitus. Biochem. Biophys. Res. Commun. 373:94–98.

Li, W., Y. Zhang, and N. Shao. 2019. Protective effect of glycine in streptozotocin-induced diabetic cataract through aldose reductase inhibitory activity. Biomed. Pharmacother. 114:108794.

Liu, L. P., T. H. Yan, L. Y. Jiang, W. Hu, M. Hu, C. Wang, Q. Zhang, Y. Long, J. Q. Wang, Y. Q. Li, M. Hu, and H. Hong. 2013. Pioglitazone ameliorates memory deficits in streptozotocin-induced diabetic mice by reducing brain β-amyloid through PPARγ activation. Acta Pharmacol. Sin. 34:455–463.

Liu, T. H., W. J. Lin, M. C. Cheng, and T. Y. Tsai. 2020. *Lactobacillus plantarum* TWK10-fermented soymilk improves cognitive function in type 2 diabetic rats. J. Sci. Food Agric. 100:5152–5161.

Lubec, G., B. Bartosch, R. Mallinger, D. Adamiker, I. Graef, H. Frisch, and H. Höger. 1990. The effect of substance L on glucose-mediated cross-links of collagen in the diabetic db/db mouse. Nephron 56:281–284.

Marthandam Asokan, S., T. Wang, W. T. Su, and W. T. Lin. 2019. Antidiabetic effects of a short peptide of potato protein hydrolysate in STZ-induced diabetic mice. Nutrients 11:779.

Natarajan Sulochana, K., S. Lakshmi, R. Punitham, T. Arokiasamy, B. Sukumar, and S. Ramakrishnan. 2002. Effect of oral supplementation of free amino acids in type 2 diabetic patients-a pilot clinical trial. Med. Sci. Monit. 8:CR131–CR137.

Niiya, Y., T. Abumiya, H. Shichinohe, S. Kuroda, S. Kikuchi, M. Ieko, S. I. Yamagishi, M. Takeuchi, T. Sato, and Y. Iwasaki. 2006. Susceptibility of brain microvascular endothelial cells to advanced glycation end products-induced tissue factor upregulation is associated with intracellular reactive oxygen species. Brain Res. 1108:179–187.

Nishitani, S., K. Takehana, S. Fujitani, and I. Sonaka. 2005. Branched-chain amino acids improve glucose metabolism in rats with liver cirrhosis. Am. J. Physiol. Gastroint. Liver Physiol. 288:1292–1300.

Nitta, A., R. Murai, N. Suzuki, H. Ito, H. Nomoto, G. Katoh, Y. Furukawa, and S. Furukawa. 2002. Diabetic neuropathies in brain are induced by deficiency of BDNF. Neurotoxicol. Teratol. 24:695–701.

Qian, Z. J., W. K. Jung, and S. K. Kim. 2008. Free radical scavenging activity of a novel antioxidative peptide purified from hydrolysate of bullfrog skin. Bioresour. Technol. 99:1690–1698.

Tu, D. G., Y. L. Chang, C. H. Chou, Y. L. Lin, C. C. Chiang, Y. Y. Chang, and Y. C. Chen. 2018. Protective effect of glycine in streptozotocin-induced diabetic cataract through aldose reductase inhibitory activity. Food Funct. 9:124–133.

U.S. Department of Agriculture (USDA), 2022. FoodData Center: chicken, liver, all classes, raw. Accessed Mar., 2022. https://fdc.nal.usda.gov/fdc-app.html#/food-details/171060/nutrients

World Health Organization (WHO), 2021. Diabetes. Accessed Nov. 2021. https://www.who.int/news-room/fact-sheets/detail/diabetes

Wu, H. C., C. Y. Shiau, H. M. Chen, and T. K. Chiou. 2003. Antioxidant activities of carnosine, anserine, some free amino acids and their combination. J. Food Drug Anal. 11:148–153.

Wu, Y. H. S., Y. L. Lin, W. Y. Yang, S. Y. Wang, and Y. C. Chen. 2021. Pepsin-digested chicken-liver hydrolysate attenuates hepatosteatosis by relieving hepatic and peripheral insulin resistance in long-term high-fat dietary habit. J. Food Drug Anal. 29:375–388.

Yaffe, K., C. M. Falvey, N. Hamilton, T. B. Harris, E. M. Simonsick, E. S. Strotmeyer, R. I. Shorr, A. Metti, and A. Schwartz. 2013. Association between hypoglycemia and dementia in a biracial cohort of older adults with diabetes mellitus. JAMA Intern. Med. 173:1300–1306.

Zafar, M., and S. N. U. H. Naqvi. 2010. Effects of STZ-induced diabetes on the relative weights of kidney, liver and pancreas in Albino rats: a comparative study. Int. J. Morphol. 28:135–142.

Zhang, S., Q. Yang, M. Ren, S. Qiao, P. He, D. Li, and X. Zeng. 2016. Effects of isoleucine on glucose uptake through the enhancement of muscular membrane concentrations of GLUT1 and GLUT4 and intestinal membrane concentrations of Na^+/glucose co-transporter 1 (SGLT-1) and GLUT2. Br. J. Nutr. 116:593–602.

Zhao, L., B. Teter, T. Morihara, G. P. Lim, S. S. Ambegaokar, O. J. Ubeda, S. A. Frautschy, and G. M. Cole. 2004. Insulin-degrading enzyme as a downstream target of insulin receptor signaling cascade: implications for Alzheimer's disease intervention. J. Neurosci. 24:11120–11126.

Zheng, Z., J. Li, and Y. Liu. 2020. Effects of partial hydrolysis on the structural, functional and antioxidant properties of oat protein isolate. Food Funct. 11:3144–3155.

Zhu, X., W. Wang, and C. Cui. 2021. Hypoglycemic effect of hydrophobic BCAA peptides is associated with altered PI3K/Akt protein expression. J. Agric. Food Chem. 69:4446–4452.